ISSN 1027-5495. Functional Materials, 29, No.1 (2022), p. 44-51.
doi:https://doi.org/10.15407/fm29.01.44

Growth mechanism, structure and thermoelectric properties of thermally evaporated $Bi_2(Te_{0.9}Se_{0.1})_3$ thin films

E.I.Rogacheva[1], S.I.Krivonogov[2], A.G.Fedorov[2], A.Yu.Sipatov[1], A.N.Doroshenko[1], O.N.Nashchekina[1], K.V.Novak[1]

[1]National Technical University "Kharkiv Polytechnic Institute",
2 Kyrpychova Str., 61002 Kharkiv, Ukraine
[2]Institute for Single Crystals, National Academy of Sciences of Ukraine,
60 Nauky Ave., 61001 Kharkiv, Ukraine

Received Deember 20, 2021

The growth mechanism, crystal structure, and morphology of thin films with thicknesses d = 16–207 nm prepared by thermal evaporation in vacuum of p–$Bi_2(Te_{0.9}Se_{0.1})_3$ polycrystal on glass substrates were studied using X-ray diffractometry and atomic force microscopy. The obtained polycrystalline thin films were single-phase and homogeneous, had a tetradymite-type structure and a unit cell parameter very close to that of $Bi_2(Te_{0.9}Se_{0.1})_3$ polycrystal but, unlike the initial polycrystal, exhibited n-type conductivity. With increasing d, the grain size and roughness of the thin films increased. It was found that the predominant direction of the crystallite growth was [0 0 l], but at d larger than ~ 130 nm, along with the reflections from the (0 0 l) planes, weak reflections from other planes appeared, indicating a certain disorientation of crystallites. An increase in d led to a monotonic increase in the Seebeck coefficient, which indicated the presence of the classical size effect. The obtained data have shown that using a low-cost method of thermal evaporation in vacuum from a single source, one can grow thin $Bi_2(Te_{0.9}Se_{0.1})_3$ films with partial Te → Se substitution in Bi_2Te_3 of a sufficiently high quality with preferential orientation [0 0 l].

Keywords: $Bi_2(Te_{0.9}Se_{0.1})_3$ polycrystal, thermal evaporation, thin film, thickness, phase composition, crystal structure, microstructure, growth direction, Seebeck coefficient.

Механізм росту, структура та термоелектричні властивості термічно випарених $Bi_2(Te_{0.9}Se_{0.1})_3$ тонких плівок. *О.І.Рогачова, С.І.Кривоногов, О.Г.Федоров, А.Ю.Сипатов, А.Н.Дорошенко, О.М.Нащокіна, К.В.Новак*

Методами рентгенівської дифрактометрії та атомно-силової мікроскопії було досліджено механізм росту, кристалічну структуру та морфологію тонких плівок товщиною d = 16–207 нм, отриманих термічним випаровуванням у вакуумі полікристала p–$Bi_2(Te_{0.9}Se_{0.1})_3$ на скляних підкладках. Отримані полікристалічні тонкі плівки були однофазними та однорідними, мали структуру типу тетрадиміту та параметр елементарної комірки, який практично збігався з параметром полікристала $Bi_2(Te_{0.9}Se_{0.1})_3$, але, на відміну від вихідного полікристала, мав n-тип провідності. Зі збільшенням d збільшувалися розміри зерен і шорсткість тонких плівок. Встановлено, що переважним напрямком росту кристалітів є [0 0 l], але зі збільшенням d вище d ~ 130 нм поряд з відбиттями від площин (0 0 l) зіявляються слабкі відбиття від інших площин, що вказує на певну дезорієнтацію кристалітів. Збільшення d призводило до монотонного збільшення коефіцієнта Зеєбека, що вказувало на наявність класичного розмірного ефекту. Отримані дані показали, що за допомогою недорогого методу термічного випаровування у вакуумі з одного джерела можна вирощувати тонкі плівки $Bi_2(Te_{0.9}Se_{0.1})_3$ з частковим заміщенням Te → Se у Bi_2Te_3 достатньо високої якості з переважною орієнтацією [0 0 l].

1. Introduction

The semiconductor compound Bi_2Te_3 and $Bi_2(Te_{1-x}Se_x)_3$ solid solutions are among the best low-temperature thermoelectric (TE) materials for cooling devices [1, 2], and this fact determines the growing interest in the study of low-dimensional structures based on them. In recent years, interest in the study of thin films of these materials has additionally increased after it was found that they have the properties of 3D-topological insulators [3, 4], in which the electrons of the surface layer obey the Dirac dispersion law and are not scattered by defects.

Bi_2Te_3 crystallizes in a rhombohedral structure (space group R3m-D^5_{3d}) [1, 2]. However, it is more common to describe its structure using a hexagonal unit cell rather than a rhombohedral one. The Bi_2Te_3 structure is formed by five-layer packets (quintets) $-Te^1-Bi-Te^2-Bi-Te^1$ (indices 1 and 2 denote different positions of Te atoms in the crystal lattice), perpendicular to the symmetry axis of the third order (a trigonal axis C_3 in a hexagonal lattice). Within each layer, identical atoms are packed into a hexagonal planar lattice, forming a dense hexagonal packing with the atoms of the underlying layers. The chemical bond within the quintets is predominantly covalent-ionic, while between the quintets, weak van der Waals forces act. This accounts for a significant anisotropy of the physical properties of Bi_2Te_3 single crystals and their low mechanical strength.

The stoichiometric Bi_2Te_3 exhibits p-type conductivity and the predominant defects are BiTe antisite defects. Bi_2Se_3, on the contrary, has an electronic type of conductivity and the prevalent defects are anion vacancies. The studies of the $Bi_2(Te_{1-x}Se_x)$F255 system have shown that when Se replaces Te in the anionic sublattice, Bi_2Te_3-based solid solutions are formed only up to $x \sim 0.15$–0.3 (the boundary composition varies across different authors), after that a second phase appears [5], and the conductivity sign changes to negative near the indicated compositions [6].

Bi_2Te_3 thin films can be obtained by various methods: thermal evaporation in vacuum from one source [7–14], thermal coevaporation from two sources [15–18], hot wall [19–21], magnetron sputtering [22], molecular beam epitaxy [23–25], etc. The growth mechanism and morphology of films, grain size, and their crystallographic orientation depend on the method of the film preparation and technological parameters. For anisotropic materials, such as Bi_2Te_3, the transport properties depend significantly on the direction in the crystal. For example, in [22], it was reported that in Bi_2Te_3 films, the predominant growth of (0 0 l) planes leads to significantly higher values of electrical conductivity and the Seebeck coefficient as compared to the predominant growth of (0 1 5) planes. Therefore, when growing films, it is important to control the preferential growth direction. In [7–11], it was shown that using the method of thermal evaporation in vacuum of Bi_2Te_3 crystals onto glass substrates and selecting optimal technological parameters, one can prepare thin polycrystalline Bi_2Te_3 films with the crystal structure of sufficiently high quality and with preferred [0 0 l] orientation of crystallites. However, the authors of earlier works [12–14], who also investigated the structure of Bi_2Te_3 thin films grown by thermal evaporation in vacuum from a single source on glass substrates, reported the preferred orientation of crystallites in the [0 1 5] direction.

In a number of works, the transport properties of films with various compositions in the Bi–Te–Se system: $Bi_2(Te_{1-x}Se_x)$ solid solutions [26–33], Bi_2Se_2Te [34], Bi_3Te_2Se [35], were investigated. However, no detailed study of the growth mechanism and structure of either monocrystalline or polycrystalline films was carried out in any of the works. Since the best TE properties in crystals were observed for $Bi_2(Te_{1-x}Se_x)$ solid solutions [36], it was interesting to find out if it is possible to grow films of these materials with a sufficiently high degree of structural perfection with [l 0 0] orientation using the method of thermal evaporation in vacuum from a single source. Only the authors of [29–33], who studied localization effects in these thin films, reported their obtaining thick polycrystalline films (d = 500–700Nnm), using $Bi_2(Te_{1-x}Se_x)$ polycrystals (x = 0.1 [30, 31] and x = 0.3 [32, 33]) as initial material, on glass substrates in the [l 0 0] orientation and with sufficiently perfect structure. The films were prepared by the hot-wall method and subjected to annealing at 500 K.

The goal of the present work was to establish whether it is possible to grow thin films in the [l 0 0] orientation, with a perfect structure and a composition close to that of the initial polycrystal $Bi_2(Te_{0.9}Se_{0.1})_3$ (in which partial replacement of Te by Se takes place). In addition, the study intended to find out what type of

conductivity the films exhibit, what are the values of the Seebeck coefficient S and whether theydepend on d.

2. Experimental

A $Bi_2(Te_{0.9}Se_{0.1})_3$ polycrystal exhibiting p-type conductivity was used as the initial material for the thin film preparation. The films with thicknesses d = 16–207 nm were grown by thermal evaporation of this polycrystal in oil-free vacuum (~ 10^{-5} Pa) and subsequent deposition onto thoroughly cleaned glass substrates heated to the temperature T_S = 500 K. The condensation rate was 0.1–0.3 nm/s. In one cycle of condensation, three holders located at different distances from the crucible with the initial material were used and this made it possible to obtain films with different but close d's and to study in more detail the dynamics of changes in the microstructure with a change in d. The film thickness and condensation rate were controlled using a calibrated quartz resonator placed near the substrates. The calibration of the resonator for d < ~ 100 nm was performed using low-angle X-ray diffraction patterns for the films by comparing experimental and computed diffraction patterns. The thickness d was varied to fit the computed curve to the experimental one. The accuracy of measuring d by the X-ray method was no worse than ~ 1.0 nm. Fig. 1 shows as an example the diffractogram of low-angle scattering for thin $Bi_2(Te_{0.9}Se_{0.1})_3$ film with d = 25 nm. For d more than ~ 100 nm, the resonator was calibrated using a MII-4 interferometer. The crystal structure, phase composition, and direction of the preferential growth were studied using XRD method and CuKα radiation. The morphology and the roughness of the film surfaces were determined using Atomic Force Microscope (AFM) Solver Pro NT-MDT with Nova legacy software. The grain size was determined by plotting the grain size distribution histograms.

The Seebeck coefficient S was measured by the compensation method relative to copper electrodes in the direction parallel to the film surface with an error not exceeding ±3 %. The types of the conductivity in the $Bi_2(Te_{0.9}Se_{0.1})_3$ polycrystal and in the films of various d were determined from the S signs.

3. Results and discussion

In Fig. 2, the diffraction patterns for the initial bulk $Bi_2(Te_{0.9}Se_{0.1})_3$ polycrystal (Fig. 2 a) and for thin films with different d prepared from this polycrystal (Fig. 2 b–f)

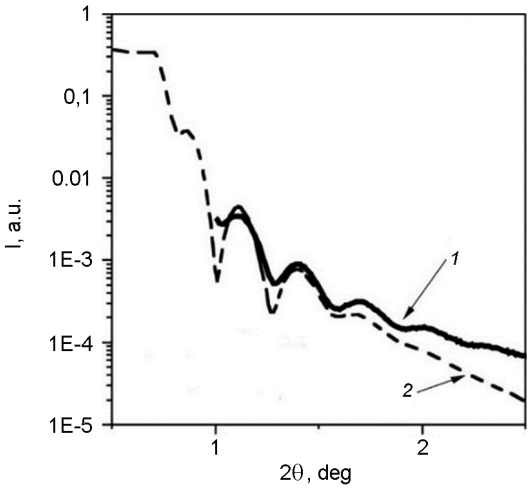

Fig. 1. Experimental (*1*) and calculated (*2*) curves of X-ray low-angle scattering for thin $Bi_2(Te_{0.9}Se_{0.1})_3$ film with thickness d = 25.0 nm.

are presented. No peaks indicating the presence of additional phases were detected. In the diffraction patterns for the films with d < ~ 130 nm, only (0 0 3), (0 0 6), (0 0 15), (0 0 18) and (0 0 21) peaks were observed along with a significant decrease in the intensity or complete disappearance of other peaks, which indicates the predominant orientation of the grains in the [0 0 l] direction. The intensity of the (0 0 l) peaks for all films with d < ~ 130 nm was practically the same, which indicates the absence of grain misorientation. However, with increasing d, in addition to the peaks from the (0 0 l) planes, the weak peaks from the (1 0 10) and (1 0 13) planes appeared. We can assume that the change in the film morphology with increasing thickness is associated with the gradual accumulation of defects in the interior of the film with increasing d. The predominant orientation of the crystallites along the C_3 axis can be explained by the peculiarities of the growth of layered structures with van der Waals bonds between the layers on amorphous substrates [20, 26]. Layers with van der Waals bonds grow parallel to the substrate, which ensures the orientation of the crystallites in the perpendicular direction [0 0 l]. A strong anisotropy of growth rates leads to more intense growth of crystallites in the direction perpendicular to the direction of the texture, which promotes rapid fusion of crystallites with each other in the film plane [1, 13]. An amorphous substrate provides a high surface mobility of atoms compared to a crystalline one, which helps to

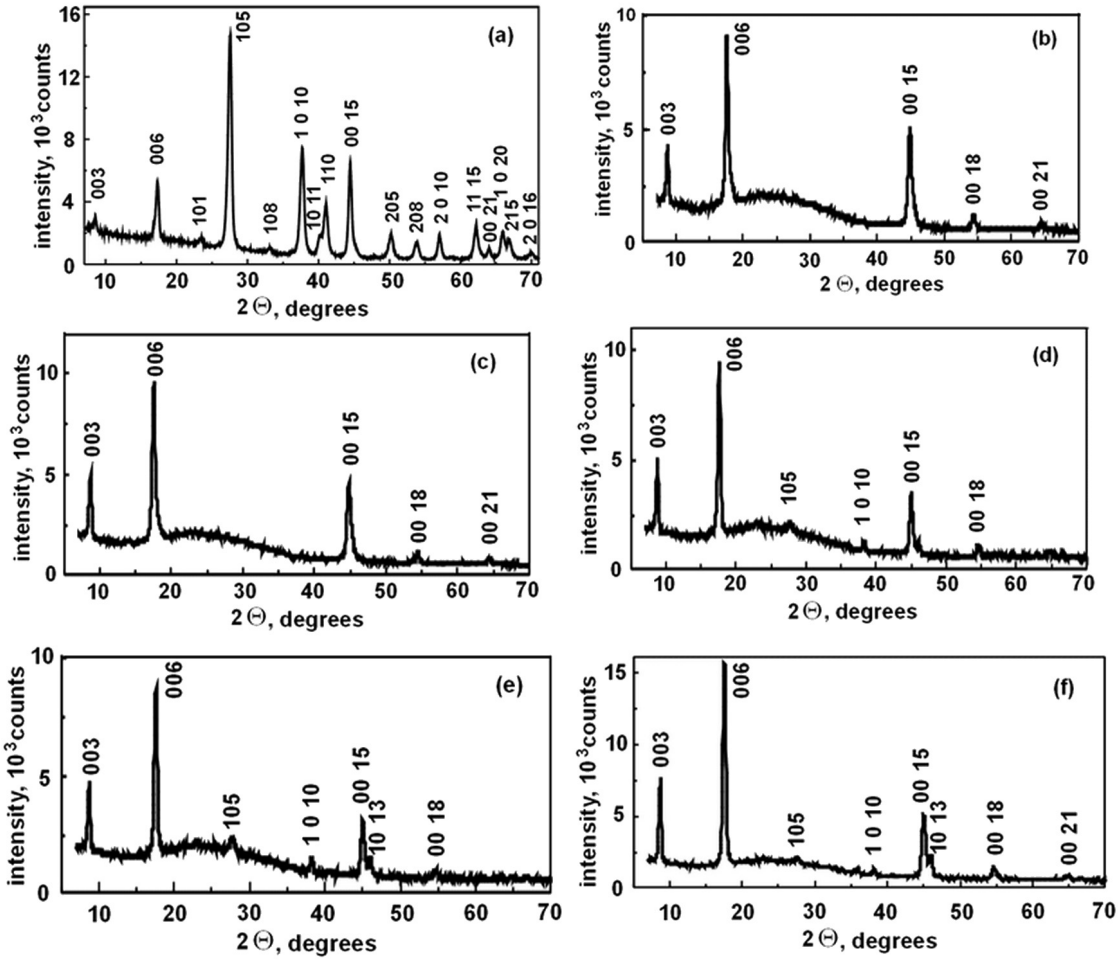

Fig. 2. X-ray diffraction patterns for the $Bi_2(Te_{0.9}Se_{0.1})_3$ bulk initial polycrystal (a) and for the thin films of the different thicknesses d prepared from this polycrystal: d = 48 nm (b), 62 нм (c), 130 nm (d), 166 nm (e), 207 nm (f).

achieve a state closer to thermodynamic equilibrium [20].

The film characterization using AFM confirmed their polycrystalline nature. The films had a pronounced granular structure without inclusions of other phases (Fig. 3). The obtained AFM images of the surface clearly show individual crystallites, having mainly a hexagonal shape, which indicates their orientation in the [0 0 l] direction perpendicular to the film surface, and this is consistent with the results of X-ray diffraction analysis (Fig. 2). Thus, from the XRD and AFM data, which are in good agreement with each other, we can conclude that in thin films prepared from the $Bi_2(Te_{0.9}Se_{0.1})_3$ polycrystal, crystallites are predominantly oriented along the [0 0 l] direction. This indicates the possibility of studying quantum effects in such films, including size effects. The grain size distribution histograms (Fig. 4, a–f), plotted on the basis of the AFM data, showed that all these histograms are fairly well approximated by the Gaussian curves corresponding to the normal distribution, when there are a large number of sources of small random errors and the center of the distribution coinciding with its maximum is the true value of the measured quantity. Based on these histograms, the dependences of the grain size D on d were plotted (Fjg. 4, f). It can be seen that increasing d leads to a growth in the grain size D. From Fig. 4, e, it is also seen that the surface roughness increases with increasing d, which, apparently, is associated with the gradual accumulation of defects both in the interior and on the surface of the film with increasing d.

The measurement of the Seebeck coefficient showed that, firstly, all films were n-type, in contrast to the initial crystal from which the films were prepared. Secondly, S changes with increasing d (Fig. 5)

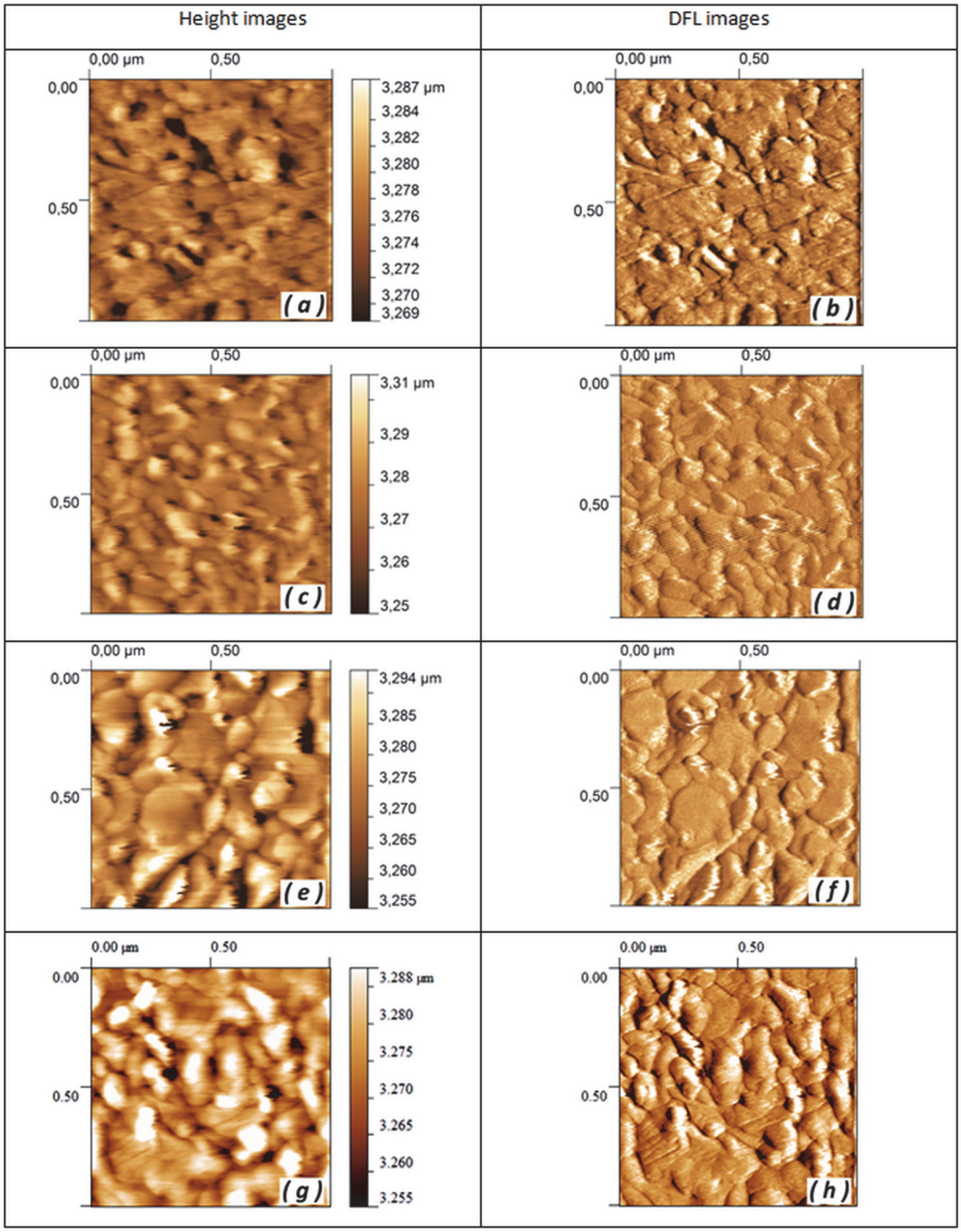

Fig. 3. AFM images recorded in contacts mode of the surfaces of the $Bi_2(Te_{0.9}Se_{0.1})_3$ thin films with thicknesses d = 48 nm: 1×1 µm (a,b), d = 62 nm: 1×1 µm (c,d), d = 130 nm: 1×1 µm (e,f), d = 207 nm: 1×1 µm (g,h). a,c,e,g — Height images, b,d,f,h — DFL images.

in the following fashion: up to ~ 75 nm, S increases very rapidly, but with a further increase in d, the rate of growth in S decreases sharply. Since usually for degenerate semiconductors, an increase in S corresponds to a decrease in the of charge carrier concentration (in this case electrons), it can be assumed that with increasing d, the electron concentration first decreases rapidly and then changes only slightly. At the same time, changes in the electronic subsystem practically do not affect the nature of changes in the microstructure with increasing d: D and h monotonically increase as d increases.

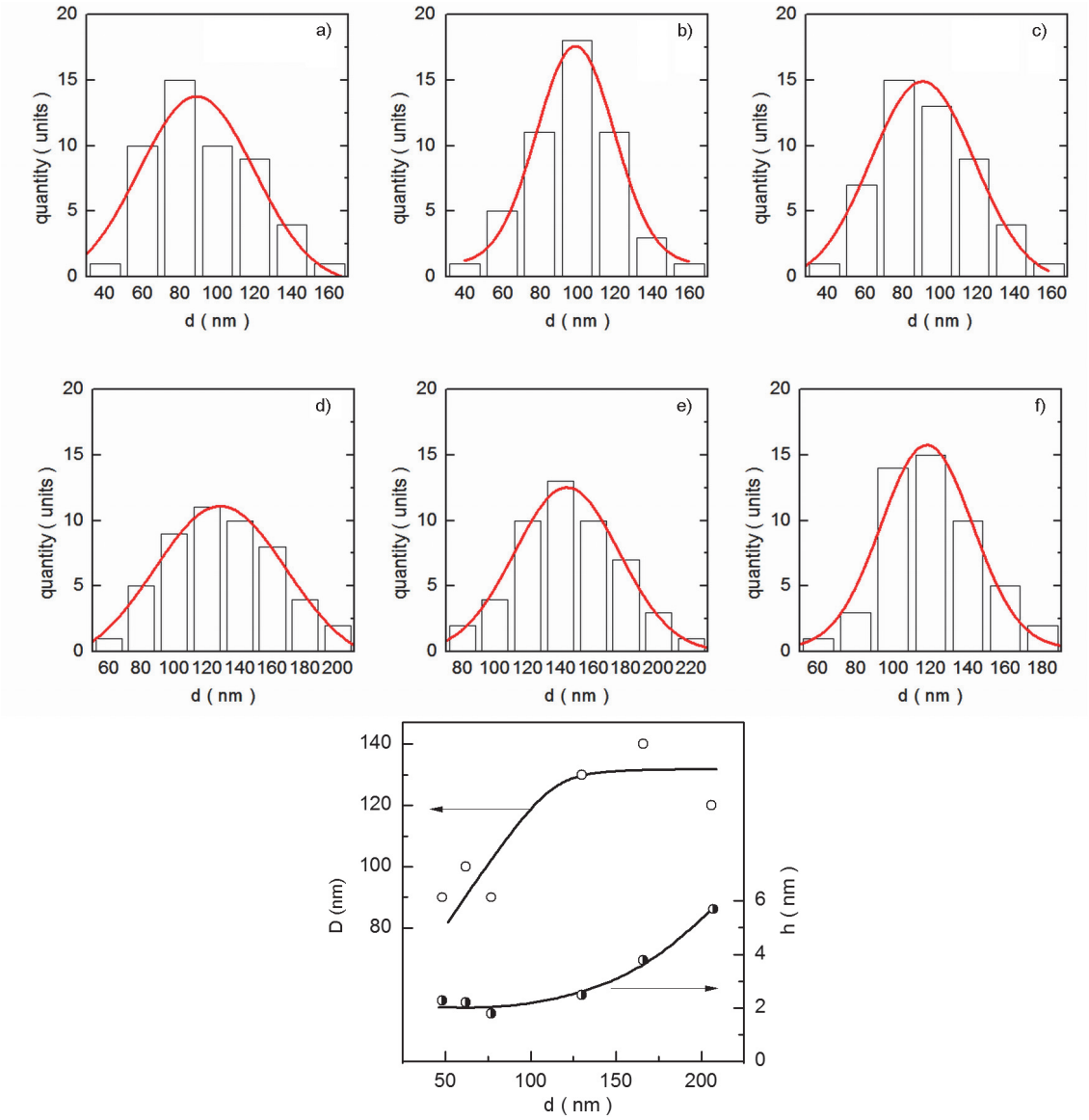

Fig. 4. Grain size distribution histograms of the $Bi_2(Te_{0.9}Se_{0.1})_3$. thin films: d = 48 nm (a), 62 nm (b), 77 nm (c), 130 nm (d), 166 (e), 207 nm (f) and grain size D and roughness h vs the film thickness d (g).

The fact that the conductivity sign in the films differs from that in the initial crystal indicates that the defect structure and type of predominant charge carriers has changed. The fact that the conductivity type changes to electronic one indicates that the predominant defects are donors. This fact may be related to several circumstances. First, as noted above, in the $Bi_2(Te_{1-x}Se_x)_3$ solid solutions based on Bi_2Te_3 in the concentration range close to the boundary of the homogeneity region, a transition from p- to n-type conductivity takes place. That is why with increasing x, a gradual change in the defect structure from the prevalence of antisite defects BiTe to the predominance of anionic vacancies, which in turn, leads to a change in the donor-acceptor ratio in the electronic subsystem and ultimately leads to an inversion of the conductivity sign from p to n. Hence, the thermodynamic state of these alloys is rather unstable, which accounts for the relative ease with which the type of conductivity changes under even a slight change in external conditions (in our case, thermal evaporation of the crystal). Second, the transition to the thin-film state is always associated with a change in the thermodynamic equilibrium conditions in a thin film

as compared to a bulk crystal, due to an increase in the contribution of the surface energy to the free energy of the crystal. And this can, with a high probability, lead to a change in the defect structure (for example, an increase in the proportion of anionic vacancies in comparison with antisite defects). Third, when a film grows, the material undergoes certain mechanical deformation, whose presence introduces additional terms to free energy associated with the deformation of the material. Let us note that the change in the conductivity type ($p \rightarrow n$) (so-called "donor-like effect") was observed by a number of authors in systems based on V_2VI_3– compounds after pressing samples, pulsed-discharge sintering of powder, hot deformation etc. [6, 27, 28, 37]. The data obtained in this work show that the donor-like effect also occurs when thin films are prepared.

Finally, it can be assumed that in the process of condensation, a change in the composition in comparison with that of the initial crystal takes place. However, the facts that the unit cell parameters of the bulk crystal and the films are the same within the limits of measurement error, that the films are homogeneous and do not contain a second phase show that possible deviations from the specified composition ($x = 0.1$) are very small and practically do not affect the microstructure.

In Fig. 5, the dependences of the Seebeck coefficient on d are presented. S increases rather rapidly with film thickness increasing up to $d \sim 75$ nm, after which the rate of increase in S slows down significantly. The increase in S with increasing d indicates the presence of the classical size effect, which occurs when d is commensurate with the mean free path of charge carriers l in the material. The classical size effect leads to a monotonic change in kinetic properties with a decrease in d due to the scattering of charge carriers at the film interfaces and an increase in the fraction of electrons scattered by the film surfaces as d decreases [20]. In crystals, the fraction of such electrons is very small and l is determined by scattering in the bulk of the sample, and in a thin film, under the condition $d \sim l$, the film thickness begins to determine l, and the surface becomes one of the types of structural imperfections.

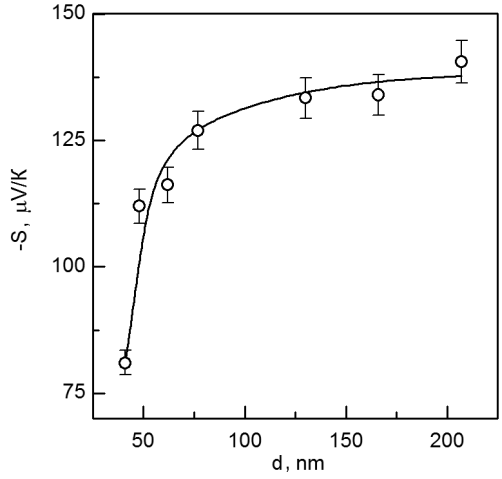

Fig. 5. The Seebeck coefficient S of the $Bi_2(Te_{0.9}Se_{0.1})_3$ thin films vs the film thickness d.

4. Conclusions

* The optimal technological parameters for obtaining thin polycrystalline $Bi_2(Te_{0.9}Se_{0.1})_3$ films with a given composition, a sufficient degree of structural perfection and a certain crystal orientation using thermal evaporation from a single source on glass substrates have been identified.

* All films obtained in this work had a rhombohedral structure and the unit cell parameter similar to that of the initial polycrystal, were homogeneous and single phase.

* The films with thicknesses d more than ~ 130 nm had a clearly pronounced [0 0 l] orientation, however, further increase in d led to the appearance of weak additional lines, indicating a slight misorientation.

* The crystallite size D increases with increasing film thickness, reaching $D \sim 140$ nm in the thickest of the studied films (d = 207 nm). The film roughness h also increases with increasing d (up to $h \sim 5.5$ nm).

* All the films obtained exhibited n-type conductivity, unlike the initial polycrystal. Possible reasons are as follows. First, the composition $x = 0.1$ in the $Bi_2(Te_{1-x}Se_x)_3$ system is close to the composition corresponding to the p–n junction point. That is why the conductivity sign can change failry easily under the influence of external factors, for example, under the transition of the material in the thin-film state. Second, a change in the thermodynamic equilibrium conditions in the thin-film state as compared to the bulk polycrystal is due to the additional contribution of the surface and the elastic stresses to the free energy of the film.

* With d increasing to ~ 75 nm, the Seebeck coefficient grows rapidly, and at d more than ~ 75 nm the rate of growth significantly slows down. The change in S with

increasing d indicates the existence of the classical size effect.

Acknowledgment. This work was supported by the Ministry of Education and Science of Ukraine (Project # M3925)

References

1. H.Scherrer, S.Scherrer, Bismuth Telluride, Antimony Telluride and their Solid Solution. In: CRC Handbook of Thermoelectric, ed. by D.M.Rowe, CRC Press, Boca Raton (1995), p.213-223.
2. L.E.Bell, *Science*, **321**, 1457 (2008). http://dx.doi.org/10.1126/science.115889
3. L.Muchler, F.Casper, B.Yan et al., *Phys. Status Solidi RRL*, **7**, 91 (2013). http://dx.doi.org/10.1002/pssr.201206411.
4. D.Culcer, *Physica E*, **44**, 860 (2012). http://dx.doi.org/10.1016/j.physe.2011.11.003.
5. O.B.Sokolov, S.Ya.Skipidarov, N.I.Duvankov, G.G.Shabunina, *J. Cryst. Growth.*, **262**, 442 (2004).
6. T.C.Chasapis, D.Koumoulis, B.Leung et al., *APL Materials*, **3**, 083601 (2015). https://doi.org/10.1063/1.4922857.
7. E.I.Rogacheva, A.V.Budnik, O.N.Nashchekina et al., *J. Electron. Mater.*, **46**, 3949 (2017). http://dx.doi.org/10.1007/s11664-017-5561-2.
8. E.I.Rogacheva, O.N.Nashchekina, A.V.Budnik et al., *Thin Solid Films*, **612**, 128 (2016). http://dx.doi.org/10.1016/j.tsf.2016.05.046
9. E.I.Rogacheva, A.V.Budnik, A.Yu.Sipatov et al., *Appl. Phys. Lett.*, **106**, 053103 (2015). https://doi.org/10.1063/1.4907319
10. E.I.Rogacheva, A.V.Budnik, A.Yu.Sipatov et al., *Thin Solid Films*, **594**, 109 (2015). 10.1016/j.tsf.2015.10.023
11. A.V.Budnik, E.I.Rogacheva, V.I.Pinegin et al., *J. Electron. Mater.*, **42**, 1324 (2013). https://doi.org/10.1007/s11664-012-2439-1
12. R.Sathyamoorthy, J.Dheepa, *J. Phys. Chem. Solids*, **68**, 111 (2007). http://dx.doi.org/10.1016/j.jpcs.2006.09.014
13. B.Jariwala, D.V.Shah, V.Kheraj, *J. Nano-Electron. Phys.*, **3**, 101 (2010). https://doi.org/10.1063/1.4732429
14. F.S.Bahabri, *Life Science Journal*, **9**, 290 (2012). https://doi.org/10.7537/marslsj090112.41
15. J.J.Lee, F.T.Schmitt, R.G.Moore et al., *Appl. Phys. Lett.*, **101**, 013118 (2012). https://doi.org/10.1063/1.4733317
16. L.M.Goncalve, C.Couto, P.Alpuim et al., *Thin Solid Films*, **518**, 2816 (2010). https://doi.org/10.1016/j.tsf.2009.08.038
17. L.W.da Silva, M.Kaviany, C.Uher, *J. Appl. Phys.*, **97**, 1 (2005). http://dx.doi.org/10.1063/1.1914948
18. H.Zou, D.M.Rowe, S.G.K.Williams, *J. Appl. Phys.*, **408**, 270 (2002). http://dx.doi.org/10.1016/S0040-6090(02)00077-9
19. J.C.Tedenac, S.Dal Corso, A.Haidoux et al., *Mat. Res. Soc. Symp. Proc.*, **545**, 93 (1998). http://dx.doi.org/ 10.1557/PROC-545-93
20. M.Ferhat, J.C.Tedenac, J.Nagao, *J. Crystal Growth*, **218**, 250 (2000). http://dx.doi.org/10.1016/S0022-0248(00)00582-0
21. M.Ferhat, B.Liautard, G.Brun et al., *J. Cryst. Growth*, **167**, 122 (1996). http://dx.doi.org/10.1016/0022-0248(96)00247-3
22. Y.Deng, Zh.Zhang, Y.Wang et al., *J. Nanopart. Res.*, **14**, 775 (2012). http://dx.doi.org/ 10.1007/s11051-012-0775-y
23. J.Numus, H.Bottner, H.Beyer et al., in: Proc. 18th Intern. Conf. on Thermoelectrics, (ICT'99), Baltimore, USA (1999), p.696. http://dx.doi.org/10.1109/ICT.1999.843481
24. J.Krumrain, G.Mussler, S.Borisova et al., *J. Crystal Growth*, **324**, 115 (2011). http://dx.doi.org/10.1016/j.jcrysgro.2011.03.008
25. J.J.Lee, F.T.Schmitt, R.G.Moore et al., *Appl. Phys. Lett.*, **101**, 013118 (2012). https://doi.org/10.1063/1.4733317
26. M.W.Oh, J.H.Son, B.S.Kim et al., *J. Appl. Phys.*, **115**, 133706 (2014) http://dx.doi.org/10.1063/1.4870818
27. T.Zhu, L.Hu, X.Zhao et al., *Adv. Sci.*, **3**, 1600004 (2016). https://doi.org/10.1002/advs.201600004
28. L.Hu, T.Zhu, X.Liu et al., *Adv. Funct. Mater.*, **24**, 5211 (2014). https://doi.org/10.1002/adfm.201400474
29. N.A.Abdullaev, S.I.Mekhtieva, N.P.Memmedov et al., *Fizika i Tekhnika Poluprovodnikov*, **44**, 853 (2010).
30. N.A.Abdullaev, N.M.Abdullaev, A.M.Kerimova et al., *Semiconductors*, **46**, 1140 (2012).
31. N.A.Abdullayev, N.M.Abdullayev, K.V.Aliquliyeva et al., *Fizika i Tekhnika Poluprovodnikov*, **47**, 586 (2013).
32. N.A.Abdullayev, A.M.Kerimova, K.V.Aliquliyeva et al., *Phys. Status Solidi C*, **12**, 822 (2015). https://doi.org/10.1002/pssc.201400338
33. R.K.Gopal, S.Singh, R.Chandra et al., *AIP Advances*, **5**, 047111 (2015). https://doi.org/10.1063/1.4917455.
34. N.A.Abdullaeva, O.Z.Alekperova, Kh.V.Aligulievaa et al., *Physics of the Solid State*, **58**, 1870 (2016). https://doi.org/10.1134/S106378341609002X.
35. P.H.Le, S.-P.Shiu, S.-R.Jian et al., *J. Alloys and Compounds*, **679**, 350 (2016). https://doi.org/10.1016/j.jallcom.2016.03.226.
36. V.A.Kutasov, L.N.Lukyanova, P.P.Konstantinov, *Fiz. Tverd. Tela*, **42**, 1985 (2000).
37. E.I.Rogacheva, E.V.Martynova, T.N.Shelest et al., *Materials Today: Proceedings*, **44**, 3506 (2019).https://doi.org/10.1016/j.matpr.2020.09.159.